

# PROCEEDINGS OF SPIE

[SPIDigitalLibrary.org/conference-proceedings-of-spie](https://SPIDigitalLibrary.org/conference-proceedings-of-spie)

## CMOS compatible design of photonic nanojet

Vincent Veluthandath, Aneesh, Senthil Murugan,  
Ganapathy

Aneesh Vincent Veluthandath, Ganapathy Senthil Murugan, "CMOS compatible design of photonic nanojet," Proc. SPIE 12152, Mesophotonics: Physics and Systems at Mesoscale, 1215203 (24 May 2022); doi: 10.1117/12.2624336

**SPIE.**

Event: SPIE Photonics Europe, 2022, Strasbourg, France

# CMOS compatible design of photonic nanojet

Aneesh Vincent Veluthandath<sup>1</sup> and Ganapathy Senthil Murugan<sup>2</sup>

Optoelectronics Research Centre, University of Southampton, SO17 1BJ, United Kingdom

## ABSTRACT

PNJs are non-resonant travelling beams with applications in enhanced Raman scattering, coupled resonator optical waveguide, high resolution microscopy, lithography and nonlinear optics. The length and beam width of the PNJ can be controlled by engineering the shape of the dielectric structure as well as by changing the refractive index contrast between the particle and the surrounding medium. The waist of PNJ moves towards the diffracting particle with increase in refractive index, and for refractive indices higher than 2, the waist is inside the particle. This migration of beam waist towards the interior of the particle is the biggest hurdle in on chip PNJ generation, because many CMOS compatible materials, including Silicon has refractive index higher than 2. In this study, we present the design and computational results of a photonic chip made of Silicon that can support PNJ outside the material boundary. We have studied the characteristics of PNJ including the width and length as well as the effect of surrounding medium.

**Keywords:** Photonic jet; nanojet; silicon photonics; microlens

## 1. INTRODUCTION

Photonic nanojet (PNJ) is a tightly focused beam of light generated at the shadow side of a mesoscale particle when illuminated by a plane-wave<sup>1,2</sup>. PNJs are non-resonant travelling beam. The beam waist of PNJ is often less than the diffraction limit and the confinement region extends more than a wavelength. Applications of PNJ includes enhanced Raman scattering<sup>3</sup>, coupled resonator optical waveguide, high resolution microscopy and lithography<sup>4</sup>. The enhanced intensity of PNJ is also used to explore nonlinear optics<sup>4</sup>. The length and beam width of the PNJ can be controlled by engineering the shape of the dielectric structure as well as by changing the refractive index contrast between the particle and the surrounding medium<sup>5</sup>. For spheres and cylinders, the waist of PNJ moves towards the particle as a function of refractive index, and for refractive indices higher than 2 the waist is inside the particle which may limit the practical applications of PNJ<sup>6</sup>. Often this becomes a limiting factor in using PNJs on chip because many CMOS compatible materials—including Silicon, GaAs, Silicon nitride—have refractive index higher than 2.

Earlier attempts to overcome this refractive index limit of 2 was relied on cleaving<sup>7</sup> or shrinking<sup>5</sup> the spherical or cylindrical particles to push the PNJs to the exterior. These structures pose difficulties in fabrication and integration into CMOS compatible platforms. Cleaved particles are also difficult to handle and difficult to align in an optical setup. Here we propose a design of a photonic chip consisting of hemi cylindrical domes of Silicon, which could be fabricated using grey scale lithography, exhibiting PNJs outside the material boundary. The PNJ generation by the proposed design was investigated using finite element methods. Numerical studies demonstrate that the proposed design support PNJ outside the Si domain and tuned by changing the radius, ellipticity and surrounding refractive index. We further observed that the intensity of the PNJ increases with increase in the radius of the hemicylinder. Length and width of PNJ also increase with increase in the radius. Our modelling also shows that the length and beamwidth of PNJ can be controlled by the eccentricity of hemicylinder. The effect of surrounding refractive index on the characteristics of the PNJ was also studied. The PNJ length and intensity increase with increase in surrounding refractive index. Width of PNJ decreases with increase in surrounding refractive index up to 1.45 and further increase broadens the PNJ.

---

<sup>1</sup> avv1a15@soton.ac.uk

<sup>2</sup> smg@orc.soton.ac.uk

## 2. ON-CHIP PHOTONIC NANOJET

The proposed design consists of a hemicylinder of Si of radius  $a$  sitting on the Si substrate. To understand the PNJ, we modeled the structure using finite element method. The refractive index of Si substrate and Si cylinder was taken as 3.4. The surrounding refractive index  $n_m$  was taken as 1. A TE polarized plane-wave was used to illuminate the hemi cylinder through the Silicon substrate. The wavelength of the light ( $\lambda$ ) is taken as 1550 nm. The radius  $a$  of the hemicylinder is taken as a multiple of the wavelength. The computational domains were terminated by perfectly matched layer. To further understand the PNJ generation, we have studied the length of PNJ ( $L_{PNJ}$ ), maximum intensity ( $I_{max}$ ) and FWHM of the PNJ as functions of the radius, surrounding refractive index and ellipticity of the hemicylinder.

### 1.1 Effect of radius of hemicylinder

Previous studies shown that, the PNJ generated by spheres and cylinder depends on the radius<sup>5,6</sup> and generally the Intensity and the length of PNJ increase with radius of curvature. To understand how our proposed design behave with change in the radius, we have varied the radius of the hemicylinder from  $2\lambda$  to  $10\lambda$ . Figure 1a shows the PNJ from a hemicylinder of radius  $a = 6\lambda$  located on silicon substrate and figure 1b shows the PNJ generated with a hemicylinder of radius  $10\lambda$ . The intensity and the length of PNJ generated by our design increase with increase in the radius of hemicylinder (figure 1c). Figure 1d shows the FWHM of PNJ as a function of the radius of hemicylinder. The FWHM increase with increase in radius.

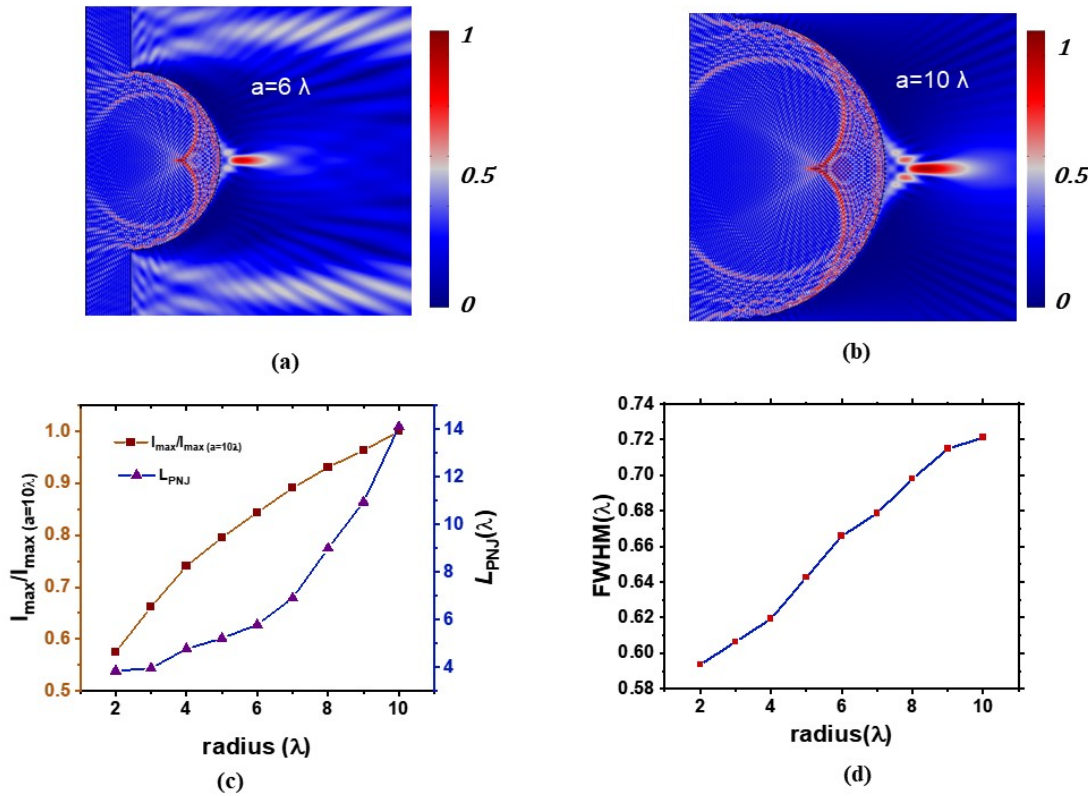


Figure 1. PNJ generated from a Si hemicylinder on a Si substrate is shown in (a-b). The radius of the hemi cylinder is  $6\lambda$  (a) and  $10\lambda$  (b). The normalized intensity and length of PNJ as a function of radius of the hemicylinder is shown in (c). FWHM as a function of radius is shown in (d).

### 1.2 Effect of ellipticity of the cylinder.

To understand how the PNJ generated by a flattened hemicylinder on the Si substrate vary as a function of the ellipticity of the hemicylinder, we have simulated a flattened hemicylinder. Figure 2a shows the geometry of the simulation. The

radius  $c$  is taken as  $5\lambda$  and  $a$  is gradually increased. Figure 2a shows the EM field intensity of PNJ of a hemicylinder  $a/c$  ratio of 0.8 and figure 2b shows the EM field intensity of a flattened hemicylinder with  $a/c$  ratio of 2.25. Figure 2c shows the normalized maximum intensity and length of PNJ as a function of  $a/c$  ratio. The maximum intensity of PNJ with  $a/c = 2.25$  is used as the normalization factor. The intensity and length of PNJ increase as the cylinder flattens. The FWHM of PNJ also increases as the cylinder is flattened (figure 2d).

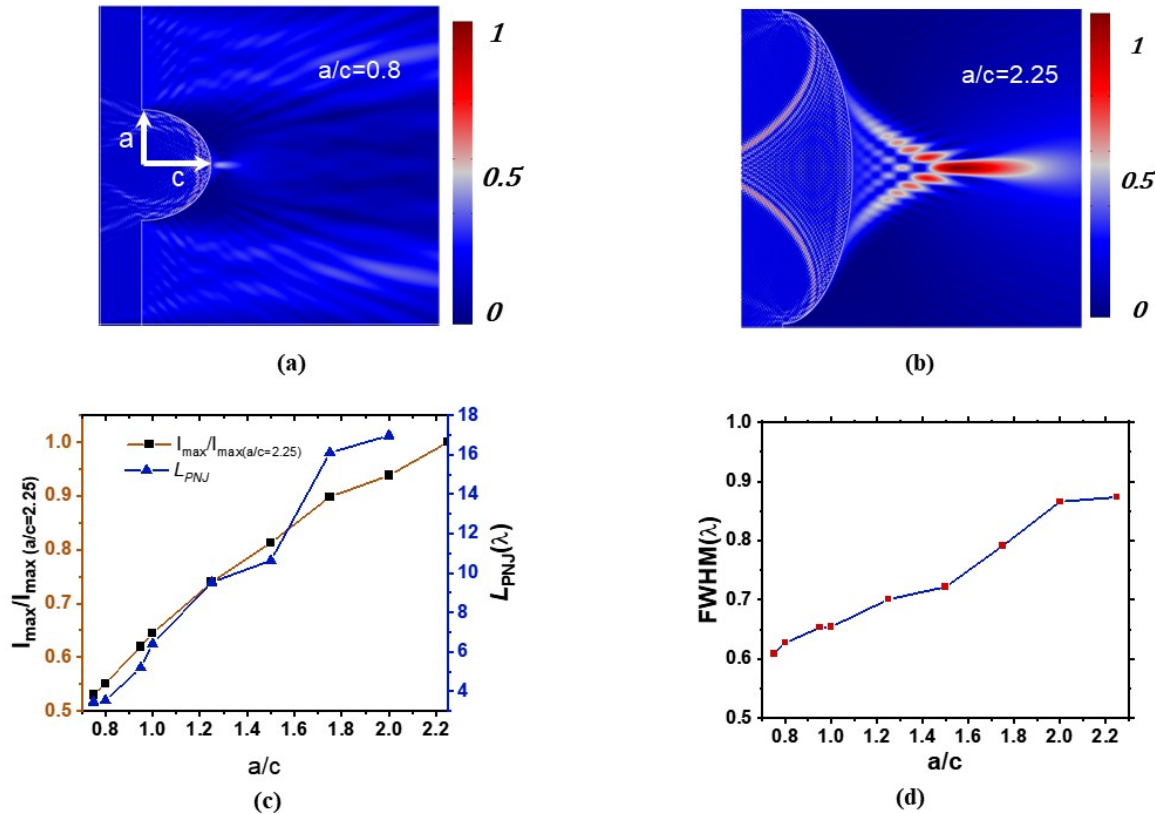


Figure 2. Variation of EM field intensity of PNJ of a hemicylinder with ellipticity  $a/c$  ratio=0.8 is shown in (a) and a flattened shape with  $a/c$  ratio=2.25 is shown in (b). The normalized intensity and length of PNJ as a function of  $a/c$  ratio is shown in (c). The variation of FWHM as a function of  $a/c$  ratio is shown in (d).

### 1.3 Effect of surrounding refractive index on the PNJ

PNJ is sensitive to the surrounding refractive index<sup>5,8</sup>. To understand the effect of surrounding refractive on the PNJ of proposed design, we have varied the refractive index of the surrounding medium from 1 to 2.1. Figure 3 shows the effect of the surrounding refractive index. The relative intensity of EM field of PNJ with surrounding refractive index  $n_m = 1$  is shown in figure 3a and  $n_m = 1.75$  is shown in figure 3b. A clear increase in intensity and length of PNJ can be observed from these figures. The normalized maximum intensity of PNJ and length of PNJ as function of surrounding refractive index is shown in figure 3c. Both Intensity and length of PNJ increase with increase in surrounding refractive index upto 1.45 and levels up after that. The FWHM decrease with increase in refractive index upto  $n_m = 1.45$  and increase if the surrounding refractive index increase above 1.45 (figure 3d).

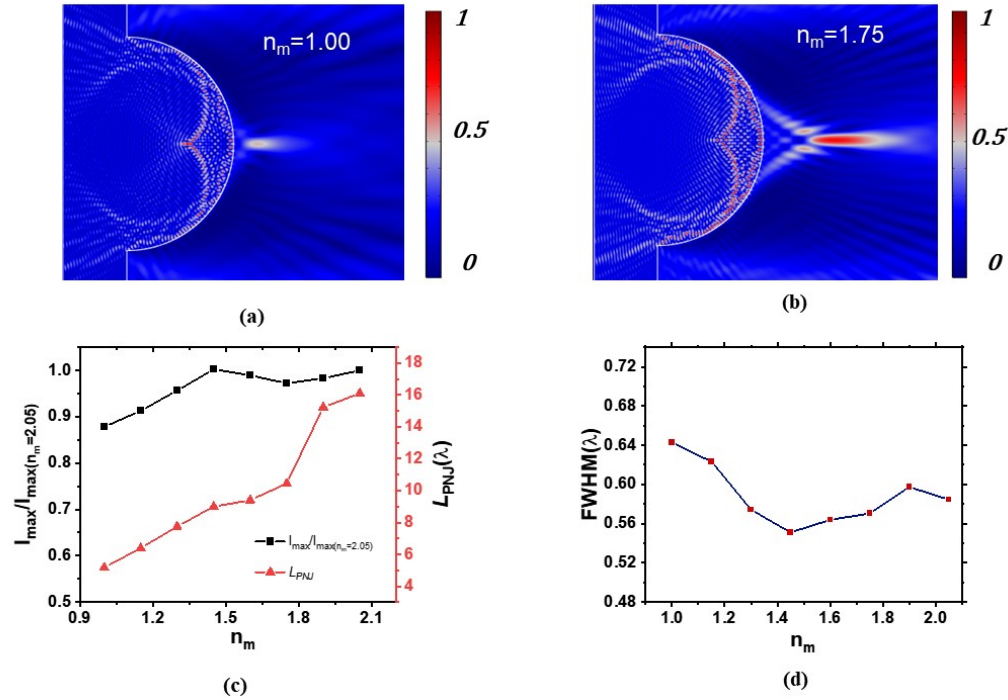


Figure 3 EM field intensity of PNJ generated with refractive index of the surrounding medium 1(a) and 1.75 (b). The Normalized intensity and the length of PNJ as function of surrounding refractive index is shown in (c). The variation of FWHM as function of surrounding refractive index is shown in (d).

### 3. CONCLUSIONS

We presented a 2D FEM study of on-chip PNJ generation in Si photonic chip. The simulations show that the hemicylindrical silicon structure placed on top of the silicon substrate support PNJ outside despite the refractive index being 3.4. The PNJs generated by the proposed structure shows an increase in intensity, length of PNJ and FWHM with increase in the radius of hemi-cylinder. We have also demonstrated that the length and intensity of PNJ can also be tuned by tuning the ellipticity the cylinder. Simulations also demonstrate the increase in surrounding refractive index leads to the elongation of PNJ. The PNJ intensity increase until the surrounding refractive index reach a value of 1.45 and stay stable after that. The FWHM of PNJ decrease with increase in surrounding refractive index upto  $n_m = 1.45$  and increase if  $n_m$  is higher than 1.45.

### ACKNOWLEDGMENT

This work was supported by the UK Engineering and Physical Sciences Research Council (EPSRC grant EP/S03109X/1 & EP/N00762X/1). The authors acknowledge the use of the IRIDIS High Performance Computing Facility, and associated support services at the University of Southampton.

## REFERENCES

- [1] Heifetz, A., Kong, S.-C., Sahakian, A. V., Taflove, A. and Backman, V., "Photonic Nanojets," *J. Comput. Theor. Nanosci.* **6**(9), 1979–1992 (2009).
- [2] Chen, Z., Taflove, A. and Backman, V., "Photonic nanojet enhancement of backscattering of light by nanoparticles: a potential novel visible-light ultramicroscopy technique," *Opt. Express* **12**(7), 1214 (2004).
- [3] Veluthandath, A. V. and Bisht, P. B., "Identification of Whispering Gallery Mode (WGM) coupled photoluminescence and Raman modes in complex spectra of MoS<sub>2</sub> in Polymethyl methacrylate (PMMA) microspheres," *J. Lumin.* **187**, 255–259 (2017).
- [4] Darafsheh, A., "Photonic nanojets and their applications," *JPhys Photonics* **3**(2), 0–21 (2021).
- [5] Gu, G., Song, J., Liang, H., Zhao, M., Chen, Y. and Qu, J., "Overstepping the upper refractive index limit to form ultra-narrow photonic nanojets," *Sci. Rep.* **7**(1), 1–8 (2017).
- [6] Luk'yanchuk, B. S., Paniagua-Domínguez, R., Minin, I., Minin, O. and Wang, Z., "Refractive index less than two: photonic nanojets yesterday, today and tomorrow [Invited]," *Opt. Mater. Express* **7**(6), 1820 (2017).
- [7] Pacheco-Peña, V. and Beruete, M., "Photonic nanojets with mesoscale high-index dielectric particles," *J. Appl. Phys.* **125**(8) (2019).
- [8] Veluthandath, A. V. and Murugan, G. S., "Photonic Nanojet Generation Using Integrated Silicon Photonic Chip with Hemispherical Structures," *Photonics* **8**(12), 586 (2021).